

Comparative Conflict Analysis between Autonomous and Human-Operated Vehicles with Pedestrians at Unsignalized Crosswalks

Andrea Avignone^{1,*†}, Marco Bassani^{2,†}, Beatrice Borgogno^{2,†}, Brunella Caroleo^{3,†},
Silvia Chiusano^{1,†} and Federico Princiotta^{3,†}

¹Dept. of Control and Computer Engineering, Politecnico di Torino, Corso Duca degli Abruzzi, 24, Torino, 10129, Italy

²Dept. of Environment, Land and Infrastructure Engineering, Politecnico di Torino, Corso Duca degli Abruzzi, 24, Torino, 10129, Italy

³LINKS Foundation, Via Pier Carlo Boggio 61, Torino, 10138, Italy

Abstract

Unsignalized crosswalks remain the most vulnerable scenario where pedestrians are exposed to the highest risks. With the imminent introduction of autonomous vehicles on public roads, safe encounters with pedestrians in these critical environments presents a significant challenge. Our study develops a rigorous methodology to quantitatively assess these dynamics in real-world mixed traffic conditions. We implemented a system that processes video data from on-street cameras to evaluate risks in vehicle-pedestrian interactions by computing key conflict measures, such as the Time-to-Collision (TTC). The analysis conducted at an unsignalized pedestrian crossing enabled a comparative evaluation between conventional and autonomous vehicles. Results highlight a higher incidence of severe conflicts in interactions with human-operated vehicles, suggesting that the cautious programming of autonomous vehicles can significantly contribute to pedestrian safety. Our findings also reveal an impact on the pedestrian decision-making process based on the type of vehicle approaching the crosswalk.

Keywords

conflict measures, autonomous vehicle, road safety, pedestrian-vehicle interaction

1. Introduction

The integration of Autonomous Vehicles (AV) into public roads represents a significant advancement in transportation technology. Although testing has been performed primarily in controlled environments [1, 2], the real challenge lies in their integration into mixed traffic conditions alongside Human-operated Vehicles (HV) and Vulnerable Road Users (VRU) [3, 4, 5, 6]. Pedestrian crossings, particularly unsignalized ones, present critical interaction points where safety concerns emerge. To quantify the severity of interactions between road users, researchers have developed Conflict Measures (CM) [7, 8]. These metrics distinguish between regular interactions and conflicts of varying magnitudes, from slight to serious, with collisions representing the most severe outcome.

Despite the prevalence of crash-based metrics, non-crash events and conflict measures provide valuable safety insights [9]. Previous studies have employed micro-simulation techniques to study AV-pedestrian interactions, but these approaches have limitations in modeling behavioral aspects and environmental factors [10]. Real-environment observations of AV-pedestrian interactions remain scarce due to high costs and legal requirements. Recent technological advances in video recording and automated analysis have facilitated safety-related event studies [11, 12, 13, 14].

SEBD 2025: 33rd Symposium on Advanced Database Systems, June 16-19, 2025, Ischia, Italy

*Corresponding author.

†These authors contributed equally.

✉ andrea.avignone@polito.it (A. Avignone); marco.bassani@polito.it (M. Bassani); beatriceborgogno@gmail.com (B. Borgogno); brunella.caroleo@linksfoundation.com (B. Caroleo); silvia.chiusano@polito.it (S. Chiusano); federico.princiotta@linksfoundation.com (F. Princiotta)

ORCID 0000-0001-7003-129X (A. Avignone); 0000-0003-2560-1497 (M. Bassani); 0000-0003-2747-9093 (B. Caroleo); 0000-0002-5740-5004 (S. Chiusano); 0000-0001-8183-4469 (F. Princiotta)



© 2025 Copyright for this paper by its authors. Use permitted under Creative Commons License Attribution 4.0 International (CC BY 4.0).

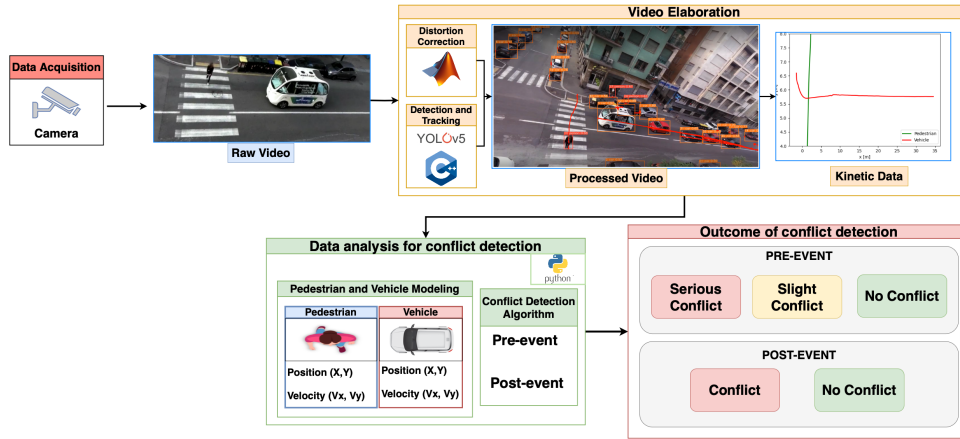


Figure 1: Proposed pipeline for conflict measure computation using videos.

This paper represents an extended abstract of a recent published work [15]. Our study investigates interactions between pedestrians and autonomous shuttles with SAE level 4 in an urban environment with dense mixed traffic in an Italian city, providing comparative insights with HV-pedestrian interactions. We propose an integrated processing pipeline for automated conflict analysis from on-street camera recordings. This pipeline includes: (i) road user detection and tracking to compute kinematic information; (ii) data analysis to model vehicle-pedestrian interactions and detect potential conflicts; (iii) conflict measures computation (e.g., Time-To-Collision) and pedestrian decision-making analysis. Our methodology moves from real-world scenarios to a more consistent representation through a vehicle box-based 2D bird’s eye view that accounts for different vehicle sizes.

2. Methodology

Fig. 1 shows the proposed pipeline with the corresponding main modules. First, the acquired videos undergo specific processing to correct distortions and apply an appropriate object detection and tracking algorithm. Once processed, trajectories and speeds are derived from the videos. Finally, potential conflicts are identified and the associated conflict measures are calculated. The pipeline supports both pre-event and post-event conflicts (e.g., Post Encroachment Time (PET)) as further explained in the original work [15]. In the following, we focus on the pre-event phase.

2.1. Video elaboration

Traffic data was collected using low-cost action cameras (Garmin VIRB, 1080p HD, 30 fps) mounted on a 10.80 m telescopic pole near a hospital area characterized by mixed vehicle types. The cameras were positioned discreetly outside the roadway to minimize driver awareness and potential behavioural modifications. The collected footage was corrected for distortion via the MATLAB Camera Calibrator App to eliminate wide-angle lens errors, which would affect the correct positioning and detected speed of users in the scene. Object detection was performed using YOLOv5 [16] with COCO classes [17] (manually labelling the autonomous shuttle since it is not part of the available classes), while StrongSORT facilitated consistent object tracking across frames [18].

For measuring spatial interactions between pedestrians and vehicles, we converted from pixels to a geo-referenced X-Y coordinate system. As reported in Fig. 2, in this system, the X-axis runs parallel to the road, while the Y-axis runs parallel to pedestrian crossings. The origin point (0,0) is located at the bottom left corner of the zebra crossing. We tracked specific reference points of the bounding boxes: for pedestrians, the center point between their feet; for vehicles, the center of the front license plate. Position tracking occurred every 34 ms.

To enhance the accuracy of spatial and motion-related variables, kinetic data is denoised using the

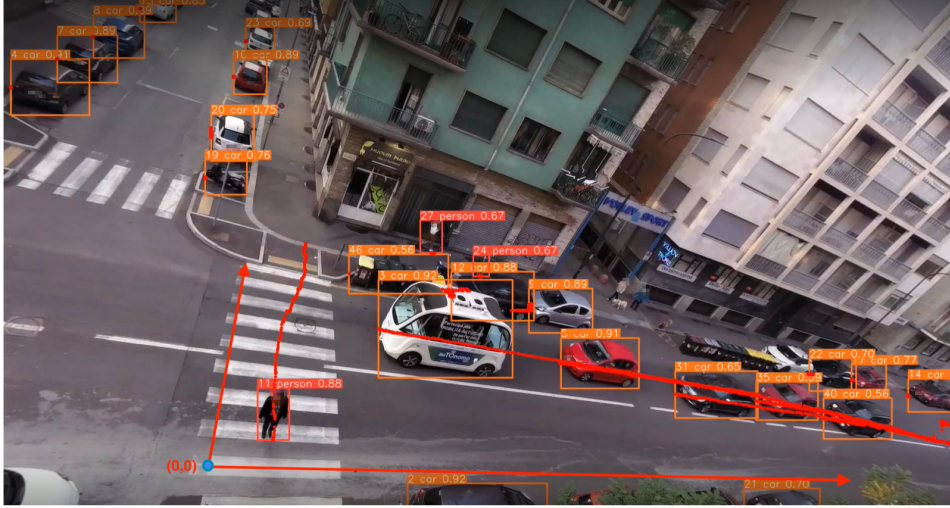


Figure 2: Complete scene with object detection and tracking during a pedestrian crossing in front of the AV.

Simple Moving Average (SMA), which mitigates noise from camera oscillation and image discretization. The SMA computes the unweighted mean over a window of k data points, given by:

$$SMA_k = \frac{1}{k} \sum_{i=n-k+1}^n p_i \quad (1)$$

where p_i is the position, n is the total number of data points, and k is the width of the window. A sensitivity analysis led to adopting $k = 30$ frames (1s), ensuring a balance between noise reduction and accuracy. Validation using AV onboard sensor data confirms the effectiveness of this approach. The estimated speed aligns closely with the recorded values, producing $R^2 = 0.95$, MAE = 0.92 km/h, and RMSE = 1.4 km/h.

2.2. Conflict Detection

After acquiring the coordinates and kinematic data, including trajectory and speed at each timestamp, we isolated the segment where the pedestrian and the AV/HV were actively engaged in an interaction. We then moved from the original camera image (Fig. 2) to the proper 2D perspective of the scene (Section 2.2.1) to analyze TTC and pedestrian decision-making (Section 2.2.2 and Section 2.2.3, respectively).

2.2.1. Vehicle and Pedestrian Modelling

The camera images and standard bounding boxes obtained with the object detection system are not adequate to simulate a 2D bird's-eye view consistent with the theoretical formulation considered. For vehicle representation, a 2D-box is positioned using the center of the frontal plate as the reference point. We established a reference catalogue of standard vehicle dimensions (Table 1) to automatically assign each detected vehicle to its corresponding box size. We applied standardized dimensions based on the vehicle type to mitigate inaccuracies due to the camera's perspective and measurement noise. The pedestrian is instead approximated as a single point in the 2D bird's-eye view, corresponding to the bottom center of the bounding box, given the difference in scale relative to vehicles.

2.2.2. Pre-event Conflict: Time-To-Collision

Interactions between road users are categorized into two types: *undisturbed passages*, where users maintain their course without altering speed or direction due to adequate spacing, and *conflicts*, which require at least one participant to take evasive action to avoid a collision. Conflicts can be classified

Table 1

Reference catalogue of standard vehicle dimensions for 2D box-based representation

| Box size | Vehicle type | | | |
|-------------------|---------------------|------|-----------------|---------|
| | Human-operated (HV) | | Autonomous (AV) | |
| | Car | Van | Bus | Shuttle |
| Length [m] | 4.50 | 5.40 | 12.20 | 4.75 |
| Height [m] | 2.00 | 2.10 | 2.55 | 2.11 |

as *minor*, where minor adjustments (such as a slight speed reduction or a shift of the trajectory) are sufficient to avoid danger, or *serious*, where a collision is inevitable unless significant evasive maneuvers are made by one or more road users [19].

Time-To-Collision (TTC) is the time that separates two road users from a collision in the pre-event phase if the collision course and speed difference are maintained [20]. Given two general Road Users RU_1 at speed V_1 and RU_2 at speed V_2 , they are on a collision course if there is at least a straight parallel to the vector of speed difference $\Delta V = V_2 - V_1$ that from the target user RU_2 intersects RU_1 . The trajectories of RU_1 and RU_2 generate a *conflicting area*: the expected place of the incident assuming that neither road user takes any evasive action. Since speed and position change over time, the *Instantaneous Time-To-Collision (ITTC)* is calculated by evaluating the TTC at each instant t . The minimum ITTC value ($ITTC_{min}$) represents the severity of the conflict, with lower values indicating a higher risk [21, 22, 23]. Based on literature [24, 25, 26], we classify $ITTC_{min} \geq 3$ s as *no conflict*, $1.5 \leq ITTC_{min} < 3$ s as *slight conflicts*, and $ITTC_{min} < 1.5$ s as *serious conflicts*. Although thresholds vary between studies, we adopt 1.5 s as the benchmark for serious conflicts, following established conventions [22, 27].

Building on the widely accepted definition of (I)TTC, this study employs a precise mathematical approach that considers, on a frame-by-frame basis, the spatial dimensions and orientation of the interacting road users, and the interaction region to determine whether the two users are on a potential collision path. Each road user (RU) is represented in a two-dimensional space by: (i) 2D box-based model showing its bird's-eye view; (ii) the RU reference point, defined by the (X, Y) coordinates of the center of the front head; (iii) two RU extreme points, represented by the highest and lowest y-coordinate values of the box.

In this work, we define the *interaction region* as the area that captures the influence of the target user's spatial occupancy on the interaction dynamics. This region is used to assess whether the two road users are on a potential collision course and whether the computation of the ITTC is feasible.

Fig. 3 illustrates the scenario of two road users, RU_1 and RU_2 , each represented by a box. When RU_2 is considered the target user, the *interaction region* is defined as the area bounded by two lines parallel to the relative velocity vector ΔV , each passing through the extreme points of RU_2 . Whether RU_1 falls within this interaction region determines whether there is a collision course between the two road users.

As illustrated in Fig. 3a, at time t_0 , RU_1 lies within the interaction region of RU_2 and thus they are on a collision course. If no evasive actions are taken, a conflict is anticipated to occur in the conflicting area after a time given by Equation 2:

$$ITTC_o = \frac{D_o}{\|\Delta V_o\|} \quad (2)$$

where D_o represents the current distance between the two road users, defined as the shortest segment parallel to ΔV (denoted ΔV_o) connecting the potential collision points P_1 and P_2 . We refer this time instant as the *Interaction Time (IT)*.

In Fig. 3b, at time t_1 , the reduction in speed of RU_1 ($V_{1,1} < V_{1,0}$) leads to a reorientation and a change in the magnitude of ΔV (here ΔV_1). As a result, the interaction region shifts and RU_1 is not included anymore. In this scenario, there is no longer a collision course, and the ITTC approaches

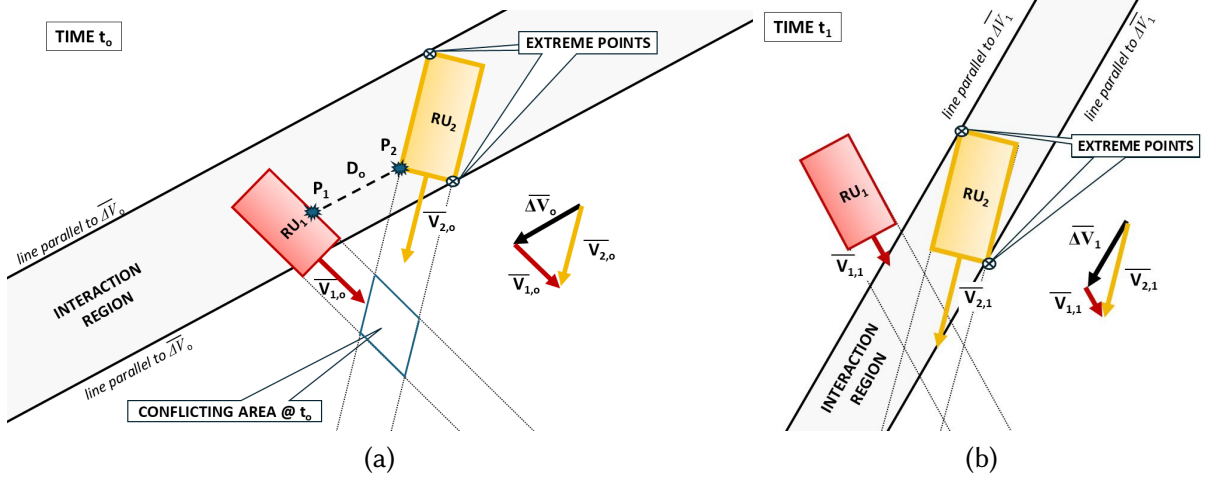


Figure 3: TTC computation framework: (a) two RUs on a collision course; (b) two RUs not on a collision course.

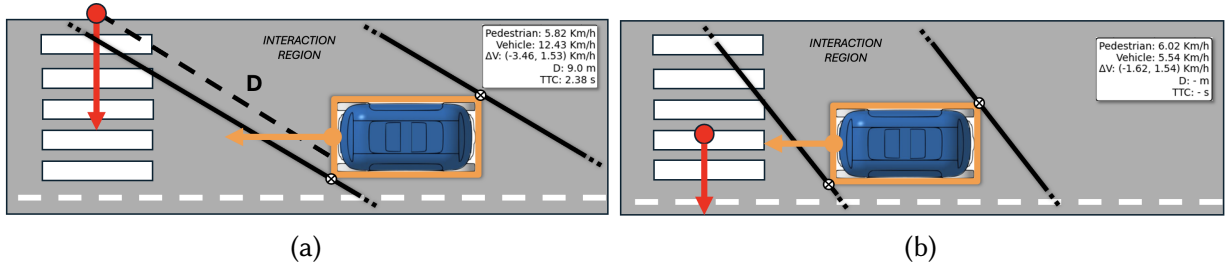


Figure 4: 2D bird's-eye view for ITTC calculation based on vehicle and pedestrian kinematic data: (a) time frame with actual conflict, (b) time frame with no detected conflict.

infinity, indicating no actual conflict. We refer to this specific time instant as the *no-Interaction Time* (no-IT).

From the collected images (see Fig. 2), our pipeline moves the view to the 2D representation of Fig. 4. We define the interaction region by two straight lines drawn at each time instant from the extreme points of the vehicle, thus the bottom-left point and top-right point. The two lines are parallel to the speed difference vector between the pedestrian and the vehicle (ΔV) and tangent to the contour of the vehicle. Upon detecting a potential conflict, the minimum distance D between the two road users along the relative velocity ΔV is computed, followed by the calculation of the ITTC according to Equation 2. An example of such a conflict scenario is shown in Fig.4a, where the pedestrian lies within the lines defined by the vehicle's contours.

This rigorous evaluation of the TTC measure instant-by-instant can produce gaps in the ITTC curve due to evasive actions, such as the pedestrian hesitations or the vehicle changes in direction or speed. Given a threshold of interest Thr_{gap} ($Thr_{gap} = 7s$ in our study) to filter the portion of interaction in which the actors are closer, we denote *Sum of no-Interaction Times* (SUM-no-IT) with Equation 3:

$$SUM\text{-no-IT} = \sum_i (\text{no-IT}_i), \quad \text{when ITTC} < Thr_{gap} \quad (3)$$

On the contrary, in Fig. 4b the road users are not in a potential collision course since the pedestrian is outside the interaction region defined by the two lines. This is due to the change in the relative velocities, which affects the slope of ΔV . This procedure provides a convenient mechanism to investigate the evolution of the whole interaction depending on the changes in speed and direction, thus identifying the most dangerous instants.

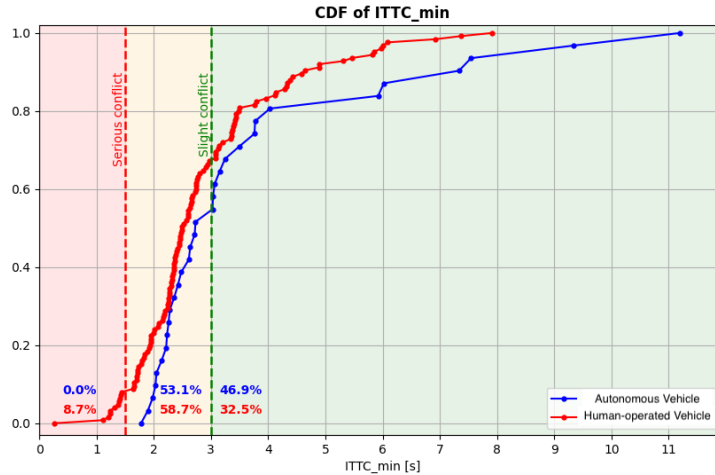


Figure 5: Cumulative Distribution Function (CDF) comparison of the $ITTC_{min}$ experimental results for HV and AV, with the percentage of interactions in each category.

2.2.3. Pre-event Conflict: Pedestrian Decision-making

Pedestrian hesitation often results from evasive manoeuvres or uncertainty in interactions with vehicles. This study examines pedestrian behaviour when crossing in mixed traffic, focusing on decision-making differences between HVs and AVs. We identify two key events based on pedestrian speed profiles [28, 29]:

- **Stop Event:** Occurs when the speed of the pedestrian drops below $Thr_{stop} = 0.3$ m/s, indicating hesitation (e.g. perceived risks or uncertainty about the intention of the vehicle).
- **Long Stop Event:** A prolonged stop exceeding $Thr_{long_stop} = 1$ s, suggesting a deliberate delay in crossing.

These thresholds, derived from literature [30, 31] and exploratory analysis, effectively capture pedestrian decision-making dynamics and manage small fluctuations in the speed estimation. Two metrics quantify these behaviors: (i) *Total Stop Time*: sum of all interruptions during a crossing; (ii) *Number of Long Stops*: count of prolonged stops. These measures provide insights into pedestrian confidence and risk perception when interacting with AVs and HVs.

3. Results

The study analyzed pedestrian-vehicle interactions at a non-signalized crosswalk along an autonomous shuttle (SAE level 4) route in an Italian city near a hospital. Video data were collected over 24 hours across eight days, focusing on one lane of a two-lane urban road to ensure data quality. A total of 168 interactions were examined, including 33 involving autonomous shuttles and 135 with human-operated vehicles, with all videos anonymized before processing.

3.1. Pre-event Analysis

The findings reveal that AV-pedestrian interactions were largely non-critical since they were predominantly within the *no conflict* range, with an $ITTC_{min}$ mean value $M = 3.66$ s, $SD = 2.278$ s. Even the lowest recorded $ITTC_{min}$ for AVs remained above the *serious conflict* threshold of 1.5s, indicating a complete absence of high-risk interactions. In contrast, HV-pedestrian interactions frequently involved actual conflicts, as their average $ITTC_{min}$ fell below the 3s ($M = 2.885$ s, $SD = 1.306$ s). The most critical case of HV recorded a significant low $ITTC_{min}$ of 0.331 s, indicating a serious safety risk. Additionally, AVs consistently prioritized pedestrian right-of-way, yielding 100% of the time, whereas HVs failed to yield in 20% of cases, highlighting an important contrast in vehicle behavior.

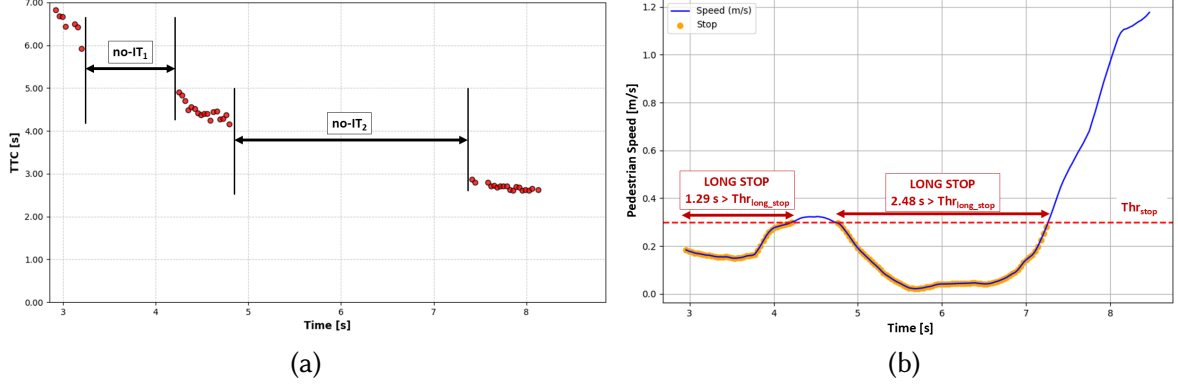


Figure 6: Example of ITTC and speed profile for pedestrian decision-making.

To compare pedestrian interactions with AVs and HVs, we analyzed the cumulative density functions (CDF) of $ITTC_{min}$ and applied the Kolmogorov-Smirnov (K-S) test. The test did not show significant differences between the two distributions ($D = 0.168$, $p = .415$), which means that they share similar characteristics. We identified the lognormal distribution as the best fit for both AV-pedestrian ($D = 0.076$, $p = .985$) and HV-pedestrian ($D = 0.110$, $p = .087$) interactions. However, Fig. 5 revealed key distinctions: AVs consistently resulted in higher $ITTC_{min}$ values, while HV interactions exhibited a more pronounced lower tail. Since lower ITTC values correspond to more dangerous interactions, the presence of critical conflicts in the HV distribution is concerning. In particular, AV interactions did not include such high-risk events, reinforcing their safer operational behavior.

3.2. Pedestrian Decision-making Behaviour

Since TTC depends on both pedestrian and vehicle speeds, the observed time gaps between interactions result from their combined dynamics. However, pedestrian-HV interactions exhibit longer average durations ($M = 1.55$ s, $SD = 1.48$ s) compared to pedestrian-AV interactions ($M = 0.94$ s, $SD = 0.75$ s), with greater variability and higher maximum values. The highest recorded gaps ($MAX = 6.53$ s for HV and $MAX = 2.31$ s for AV) can suggest evasive actions. To better understand pedestrian decision-making, we analyze stop patterns and speed variations during crossings (see Section 2.2.3). Stops, especially at the start of crossings, indicate hesitation and uncertainty. Pedestrians interacting with AVs tend to have shorter and more consistent stop durations, reflected in a narrower interquartile range ($IQR_{AV} = 0.204$ s) compared to HV interactions, which show greater variability ($IQR_{HV} = 0.99$ s) and extreme outliers up to 5.7 s. Also, *Long Stops* (1 s) occur in 12.12% of AV interactions versus 23.53% for HVs. Only for HVs, we have observed cases with multiple long stops for the same interaction. This suggests that HVs, with their less predictable behavior, induce more hesitation; while AVs facilitate more confident and predictable pedestrian crossings.

As an example, Fig.6 captures a pedestrian's decision-making process during a pedestrian-HV interaction, depicting ITTC evolution (Fig.6a) alongside speed variations (Fig. 6b). At the start of the crossing, two prolonged stops emerge, marking moments of hesitation as the pedestrian evaluates whether to proceed. These pauses correspond with extended *no-Interaction Times*, as seen in the ITTC curve, where the pedestrian either slows significantly or comes to a full stop, thus showing signs of uncertainty. This pattern underscores that the most critical moments of indecision occur at the beginning of crossings, when pedestrians assess potential risks. Long stops are not only affected by the pedestrian's own judgment but also by the vehicle's responsiveness. This dynamic is especially relevant at uncontrolled crossings, where yielding behavior is uncertain and influences pedestrian confidence in proceeding.

4. Conclusions

The introduction of AVs in mixed traffic must be carefully evaluated to ensure safety. This study analyzed real-world pedestrian-vehicle interactions, demonstrating that AVs exhibit a lower collision risk than HVs with safer interactions at unsignalized crosswalks. Using the proposed pipeline to build a rigorous top-view 2D representation of the scene, we extracted spatial-temporal trajectories and computed conflict measures, revealing safer interactions with AVs, which consistently yielded to pedestrians with respect to HVs. Pedestrian behavior varied depending on vehicle type: interactions with HVs involved longer hesitation and stops, while AVs' predictable behavior fostered smoother crossings. However, the conservative approach of the AVs, including waiting until the crosswalk was completely clear, can impact traffic flow. AV settings should be optimized to balance safety and efficiency, adapting speed and acceleration based on local traffic dynamics. Our findings provide valuable insights for AV integration, offering data for micro-simulations and informing both transport operators and AV providers on optimal deployment strategies.

Future research could extend this study to more complex crosswalk designs, incorporating factors like multiple lanes, median refuges, or advanced warning systems. Additionally, the proposed methodology could be applied to a broader range of interactions involving vulnerable road users and diverse environmental conditions, such as nighttime crossings or even different countries, to enhance its generalizability. As urban mobility shifts towards eco-friendly modes like bikes and scooters, their distinct traffic dynamics introduce new safety challenges. Investigating interactions between autonomous shuttles and these road users could provide valuable insights into the risks and benefits of smart mobility solutions.

Acknowledgments

This work was partially supported by the funding from the European Union's Horizon 2020 research and innovation programme under grant agreement No 875530 (SHOW); and partially supported by the SmartData@PoliTO center on Big Data and Data Science.

Declaration on Generative AI

The author(s) have not employed any Generative AI tools.

References

- [1] E. Chaalal, C. Guerlain, E. Pardo, S. Faye, Integrating connected and automated shuttles with other mobility systems: Challenges and future directions, *IEEE Access* 11 (2023) 83081–83106. doi:10.1109/ACCESS.2023.3294110.
- [2] S. Razmi Rad, H. Farah, H. Taale, B. van Arem, S. P. Hoogendoorn, Design and operation of dedicated lanes for connected and automated vehicles on motorways: A conceptual framework and research agenda, *Transportation Research Part C: Emerging Technologies* 117 (2020) 102664. URL: <https://www.sciencedirect.com/science/article/pii/S0968090X20305799>. doi:<https://doi.org/10.1016/j.trc.2020.102664>.
- [3] A. Parks-Young, G. Sharon, Intersection management protocol for mixed autonomous and human-operated vehicles, *IEEE Transactions on Intelligent Transportation Systems* 23 (2022) 18315–18325. doi:10.1109/TITS.2022.3169658.
- [4] M. Barthauer, B. Friedrich, Presorting and presignaling: A new intersection operation mode for autonomous and human-operated vehicles, *Transportation Research Procedia* 37 (2019) 179–186. URL: <https://www.sciencedirect.com/science/article/pii/S2352146518305969>. doi:<https://doi.org/10.1016/j.trpro.2018.12.181>, 21st EURO Working Group on Transportation Meeting, EWGT 2018, 17th – 19th September 2018, Braunschweig, Germany.

- [5] M. Wu, H. Jiang, C.-A. Tan, Automated parking space allocation during transition with both human-operated and autonomous vehicles, *Applied Sciences* 11 (2021). URL: <https://www.mdpi.com/2076-3417/11/2/855>. doi:10.3390/app11020855.
- [6] R. Gasper, S. Beutelschieß, M. Krumnow, L. Simon, Z. Baksa, J. Schwarzer, Simulation of autonomous roboshuttles in shared space, *EPiC Series in Engineering* 2 (2018) 183–193.
- [7] A. Tarko, *Measuring road safety with surrogate events*, Elsevier, 2019.
- [8] L. Zheng, T. Sayed, F. Mannering, Modeling traffic conflicts for use in road safety analysis: A review of analytic methods and future directions, *Analytic Methods in Accident Research* 29 (2021) 100142. URL: <https://www.sciencedirect.com/science/article/pii/S2213665720300324>. doi:<https://doi.org/10.1016/j.amar.2020.100142>.
- [9] A. Lareshyn, T. De Ceunynck, C. Karlsson, Åse Svensson, S. Daniels, In search of the severity dimension of traffic events: Extended delta-v as a traffic conflict indicator, *Accident Analysis & Prevention* 98 (2017) 46–56. URL: <https://www.sciencedirect.com/science/article/pii/S0001457516303566>. doi:<https://doi.org/10.1016/j.aap.2016.09.026>.
- [10] A. Papadoulis, M. Quddus, M. Imprialou, Evaluating the safety impact of connected and autonomous vehicles on motorways, *Accident Analysis & Prevention* 124 (2019) 12–22. URL: <https://www.sciencedirect.com/science/article/pii/S0001457518306018>. doi:<https://doi.org/10.1016/j.aap.2018.12.019>.
- [11] A. H. Kalantari, Y. Yang, J. Garcia de Pedro, Y. M. Lee, A. Horrobin, A. Solernou, C. Holmes, N. Merat, G. Markkula, Who goes first? a distributed simulator study of vehicle–pedestrian interaction, *Accident Analysis & Prevention* 186 (2023) 107050. URL: <https://www.sciencedirect.com/science/article/pii/S0001457523000970>. doi:<https://doi.org/10.1016/j.aap.2023.107050>.
- [12] E. Beauchamp, N. Saunier, M.-S. Cloutier, "Study of automated shuttle interactions in city traffic using surrogate measures of safety", Elsevier, *Transportation Research Part C* 135 (2022). URL: <https://doi.org/10.1016/j.trc.2021.103465>.
- [13] D. Yang, K. Ozbay, K. Xie, H. Yang, F. Zuo, D. Sha, Proactive safety monitoring: A functional approach to detect safety-related anomalies using unmanned aerial vehicle video data, *Transportation Research Part C: Emerging Technologies* 127 (2021) 103130. URL: <https://www.sciencedirect.com/science/article/pii/S0968090X21001492>. doi:<https://doi.org/10.1016/j.trc.2021.103130>.
- [14] R. Madigan, S. Nordhoff, C. Fox, R. E. Amini, T. Louw, M. Wilbrink, N. Merat, "Understanding interaction between Automated Road Transport System and other road users: A video analysis", Elsevier, *Transportation Research Part F* 66 (2019) 196–213. URL: <http://doi.org/10.1016/j.trf.2019.09.006>.
- [15] A. Avignone, M. Bassani, B. Borgogno, B. Caroleo, S. Chiusano, F. Princiotta, Evaluating unsignalized crosswalk safety in the age of autonomous vehicles, *Computers in Industry* 167 (2025) 104259. URL: <https://www.sciencedirect.com/science/article/pii/S0166361525000247>. doi:<https://doi.org/10.1016/j.compind.2025.104259>.
- [16] J. Redmon, S. Divvala, R. Girshick, A. Farhadi, You only look once: Unified, real-time object detection, in: *2016 IEEE Conference on Computer Vision and Pattern Recognition (CVPR)*, 2016, pp. 779–788. doi:10.1109/CVPR.2016.91.
- [17] T.-Y. Lin, M. Maire, S. Belongie, L. Bourdev, R. Girshick, J. Hays, P. Perona, D. Ramanan, C. L. Zitnick, P. Dollár, Microsoft coco: Common objects in context, 2015. [arXiv:1405.0312](https://arxiv.org/abs/1405.0312).
- [18] Y. Du, Z. Zhao, Y. Song, Y. Zhao, F. Su, T. Gong, H. Meng, Strongsort: Make deepsort great again, 2023. [arXiv:2202.13514](https://arxiv.org/abs/2202.13514).
- [19] C. Hydén, The development of a method for traffic safety evaluation: The swedish traffic conflicts technique, Lund Institute of Technology, Department of Traffic Planning and Engineering (1987).
- [20] C. Hydén, Traffic conflicts technique: state-of-the-art, *Traffic Safety Work with Video-processing*, Green Series, 43, University Kaiserslautern. Transportation Department (1996).
- [21] A. Tarko, "Measuring Road Safety with Surrogate Events", Elsevier (2019).
- [22] A. Arun, M. M. Haque, A. Bhaskar, S. Washington, T. Sayed, A systematic mapping review of surrogate safety assessment using traffic conflict techniques, *Accident Analysis & Prevention*

- 153 (2021) 106016. URL: <https://www.sciencedirect.com/science/article/pii/S0001457521000476>. doi:<https://doi.org/10.1016/j.aap.2021.106016>.
- [23] R. Ezzati Amini, K. Yang, C. Antoniou, Development of a conflict risk evaluation model to assess pedestrian safety in interaction with vehicles, *Accident Analysis & Prevention* 175 (2022) 106773. URL: <https://www.sciencedirect.com/science/article/pii/S0001457522002081>. doi:<https://doi.org/10.1016/j.aap.2022.106773>.
- [24] E. Sacchi, T. Sayed, P. deLeur, A comparison of collision-based and conflict-based safety evaluations: The case of right-turn smart channels, *Accident Analysis & Prevention* 59 (2013) 260–266. URL: <https://www.sciencedirect.com/science/article/pii/S0001457513002303>. doi:<https://doi.org/10.1016/j.aap.2013.06.002>.
- [25] E. Sacchi, T. Sayed, Conflict-based safety performance functions for predicting traffic collisions by type, *Transportation Research Record* 2583 (2016) 50–55. URL: <https://doi.org/10.3141/2583-07>. doi:10.3141/2583-07. arXiv:<https://doi.org/10.3141/2583-07>.
- [26] K. El-Basyouny, T. Sayed, Safety performance functions using traffic conflicts, *Safety Science* 51 (2013) 160–164. URL: <https://www.sciencedirect.com/science/article/pii/S0925753512001671>. doi:<https://doi.org/10.1016/j.ssci.2012.04.015>.
- [27] D. Gettman, L. Pu, T. Sayed, S. G. Shelby, S. Energy, et al., Surrogate safety assessment model and validation, Technical Report, Turner-Fairbank Highway Research Center, 2008.
- [28] M. Jay, A. Régnier, A. Dasnon, K. Brunet, M. Pelé, The light is red: Uncertainty behaviours displayed by pedestrians during illegal road crossing, *Accident Analysis & Prevention* 135 (2020) 105369. URL: <https://www.sciencedirect.com/science/article/pii/S0001457519303082>. doi:<https://doi.org/10.1016/j.aap.2019.105369>.
- [29] P. Onelcin, Y. Alver, The crossing speed and safety margin of pedestrians at signalized intersections, *Transportation Research Procedia* 22 (2017) 3–12. URL: <https://www.sciencedirect.com/science/article/pii/S2352146517301369>. doi:<https://doi.org/10.1016/j.trpro.2017.03.002>, "19th EURO Working Group on Transportation Meeting, EWGT2016, 5-7 September 2016, Istanbul, Turkey".
- [30] R. Noland, Behavioural issues in pedestrian speed choice and street crossing behaviour: A review, *Transport Reviews* 28 (2008) 61. doi:10.1080/01441640701365239.
- [31] M. M. Ishaque, R. B. Noland, Behavioural issues in pedestrian speed choice and street crossing behaviour: A review, *Transport Reviews* 28 (2008) 61–85. URL: <https://doi.org/10.1080/01441640701365239>. doi:10.1080/01441640701365239. arXiv:<https://doi.org/10.1080/01441640701365239>.